

Ecofriendly-developed Polyacrylic Acid-coated Magnetic Nanoparticles as Catalysts in Photo-fenton Processes

Laura M. Sanchez^{1,*}, Pablo A. Ochoa Rodríguez², Daniel G. Actis³, Verónica R. Elías², Griselda A. Eimer², Verónica Lassalle⁴, Vera A. Alvarez¹

¹Materiales Compuestos Termoplásticos (CoMP), Instituto de Investigaciones en Ciencia y Tecnología de Materiales (INTEMA), CONICET - Universidad Nacional de Mar del Plata (UNMDP). Av. Colón 10890, Mar del Plata, 7600, Argentina

²Centro de Investigación y Tecnología Química (CITeQ) (UTN-CONICET), Facultad Regional Córdoba, Maestro López y Cruz Roja Argentina, Ciudad Universitaria, CP: 5016 Córdoba, Argentina

³Instituto de Física de La Plata (IFLP), CONICET-Departamento de Física, Universidad Nacional de La Plata (UNLP). La Plata, 1900, Argentina

⁴INQUISUR, Departamento de Química, Universidad Nacional del Sur (UNS)-CONICET, Av. Alem 1253, 8000 Bahía Blanca, Argentina

*Corresponding author: E-mail: lsanchez@mdp.edu.ar; Tel.: (+54) 223 6260600

DOI: 10.5185/amlett.2020.031486

In this work, iron oxide-based magnetic nanoparticles (MNPs) stabilized by polyacrylic acid (PAA) polymer were prepared and characterized as a continuation of a previous research already reported. MNPs composed by pure magnetite cores having good magnetic properties were developed, thus achieving an improvement in the modified coprecipitation method used. The photocatalytic activity of the nanoparticles towards acid orange 7 (AO7), under both radiation types, UV-Vis and LED-Vis, was tested. Pollutant degradation percentages of 64 and 37 % were obtained by using UV-Vis and LED-Vis radiation, respectively.

Introduction

Due to the increase in water contamination by refractory and persistent substances of anthropic origin, such as heavy metals, metalloids, biocides, and emerging pollutants (pharmaceutical products, endocrine disruptors, nitrosamines) different studies are being made currently in order to respond to this issue. These investigations are related to a growing concern that began with United Nations Organization announcement, to include drinking water and its sanitation as a fundamental right, and incorporating it as a Sustainable Development Goal within the 2030 Agenda. Considering that the mentioned substances cannot be treated with conventional methods, Advanced Oxidation Processes are presented as simple, efficient and economical techniques of great utility for the removal of contaminants in water, air and soil. The objective is to destroy organic matter, promoting the degradation and mineralization of pollutants. These processes, such as heterogeneous photocatalysis, the Fenton and Photo-Fenton processes, are based on the formation of highly reactive species, such as the radical $\cdot\text{OH}$, capable to oxidize most of the organic compounds [1].

In particular, heterogeneous photocatalysis is based on the irradiation of a semiconductor solid with certain energy, with the purpose of generating e^-/h^+ pairs in the conduction and valence bands. When these pairs migrate to the surface and react with other species in the reaction medium, the radicals are formed and attach to pollutants [2].

While TiO_2 is one of the most used materials as a photocatalyst, in recent years, the use of nano-particulated iron materials of the magnetite type ($n\text{Fe}_3\text{O}_4$) in oxidation processes along with adsorption and co-precipitation synthesis methods application, has acquired great interest in pollutant treatment processes. The main advantages in the use of these nanoparticles are their relative low cost, availability, low toxicity, and biodegradability [3].

Photocatalytic degradation of pollutants is mainly achieved through the application of conventional ultraviolet lamps, which are mainly mercury vapor lamps (whether of low, medium, or high pressure). They have a relatively high energy consumption, contain hazardous mercury, require cooling, have a relatively short life-span, and can be difficult to operate. Recently, solid state technology has led to the development of compact, lower cost, and environmentally friendly light emitting diodes (LEDs). Some advantages of using LEDs are their small size and relatively long life span compared to conventional ultraviolet sources. Traditional UV sources have mainly been used in UV curing, disinfection, sensor, and photocatalysis applications. However, LEDs have recently been recognized as an alternative to conventional UV irradiation sources [4,5].

Several iron oxide-based photocatalysts have been recently used in Photo-Fenton processes, including biosynthesized iron oxide nanoparticles and other ones being incorporated onto multi-walled carbon nanotubes, in layered double hydroxides, in diamond nanoparticles, anatase TiO_2 and combined with SiO_2 to generate magnetic

double-mesoporous-shelled hollow spheres [6-11]. In this work, iron oxide-based magnetic nanoparticles (MNPs) stabilized by polyacrylic acid (PAA) polymer were prepared and characterized as a continuation of a previous research already reported [12]. The PAA was employed to stabilize the developed MNPs by providing steric and electrostatic repulsion against particle aggregation [12,13]. Then, the photocatalytic activity of the nanoparticles, under both radiation types, UV-Vis and LED-Vis, was tested. At the same time, acid orange 7 (AO7) was chosen as model pollutant. At this point it is important to note that dyes molecules usually found in textile industries wastewater effluents are resistant to conventional treatments and therefore are classified as recalcitrant pollutants. In this sense, the efficiency of the AOPs applied for their treatment is very susceptible to the effluent conditions. Considering that it is very difficult to simulate the characteristics of a real effluent it results almost no possible to duplicate the conditions of wastewater properties due to they vary significantly even for the same industry. Therefore, the aim of this work is to present a catalytic evaluation of magnetic and stable nanoparticles synthesized by a novel and simple method, as a first approach on the applicability of these as catalysts for dye treatment. Then, a pH and AO7 concentration usually found in real industries was simulated. In future works it will be present the study of the magnetic particles efficiency under real effluent conditions.

Experimental

Materials

For iron oxide MNPs preparation two different iron salts were used as starting materials: $\text{FeSO}_4 \cdot 7\text{H}_2\text{O}$ and $\text{FeCl}_3 \cdot 6\text{H}_2\text{O}$ (both from Cicarelli Laboratory, Argentina). Regarding the PAA, a Mw 5000 g/mol starting material purchased from Polysciences was employed. Other reactants were also incorporated: NaOH (Biopack, Argentina) and bidistilled water.

Magnetic nanoparticles synthesis

PAA-coated MNPs were prepared through coprecipitation method, according to a previously reported procedure [12], but including some modifications such as the replacement of NH_4OH and N_2 atmosphere by NaOH and air atmosphere, respectively. Briefly, 4.75 g of $\text{FeCl}_3 \cdot 6\text{H}_2\text{O}$ and 2.45 g of $\text{FeSO}_4 \cdot 7\text{H}_2\text{O}$ were dissolved in 80 mL of milli-Q water at 60 °C. Then, the PAA was added to the system (0.6 g) and vigorous stirring was maintained for 30 min. After this, the solution was dropped onto a NaOH solution (5M), resulting in an instantaneous color change from orange to black.

Characterizations

In order to determine the qualitative and quantitative compositions of the sample, X-ray Diffraction Analysis (XRD), Fourier Transformed Infrared Spectroscopy (FTIR)

and Thermogravimetric (TGA) measurements were done. For this, samples were dried in an oven at 25 °C until constant weight. TGA was conducted in a TA-Q500 equipment from room temperature to 800°C under N_2 atmosphere at a heating rate of 10°C/min. XRD measurements took place in an Analytical Expert Instrument for 2θ values from 10 to 65 degrees at a rate of 2°/min. For this, monochromatic Cu-K α radiation was employed. In the case of FTIR measurements, they were done in attenuated total reflectance modes (smart Orbit ATR accessory) in a Thermo Scientific Nicolet 6700 spectrometer, employing a resolution of 4 cm^{-1} , from 400 to 4000 cm^{-1} .

In order to determine the MNPs sizes, sizes distribution, morphology and superficial charges, dynamic light scattering (DLS) and transmission electron microscopy (TEM) measurements were done. The hydrodynamic particle diameters, size distribution and zeta potential were measured by DLS in a Malvern Zetasizer equipment at room temperature. Dispersions of the dried MNPs were prepared in NaCl (0.01 M) water solutions. For zeta potential determinations (from pH 3 to 9) the Smoluchowski equation was used. Some of the prepared MNPs were observed by TEM to examine the respective morphologies in a JEOL100-CX II-Japan (CRIBABB – CCT - Bahía Blanca, Argentina). For this measurement, MNPs suspensions were prepared by using ethanol-water solutions (50% - 50%).

Finally, measurements of magnetization of the PAA-coated MNPs were also done. For this, VSM magnetometry was used. 42.7(1) mg of the dry MNPs were measured at room temperature as a function of the applied magnetic field between from -19 kOe to 19 kOe.

Water remediation tests

Regarding degradation experiments under UV-VIS radiation, they were performed in a photoreactor consisted of a borosilicate glass tube of 0.85 L. Four UV-Vis lamps (Actinic BL 20 W, Philips) were placed around the tube. These lamps emit a continuum spectrum in the wavelength range between 350 and 400 nm and two bands at 404 and 438 nm. For temperature control, a tube was placed in the center of the reactor allowing the circulation of refrigeration water. A circulation pump and a thermo stated water bath were used for this purpose. The suspension volume employed in the experiments was 0.5 L with an initial concentration of the AO7 and the catalyst of 20 mg/L and 1 g/L, respectively.

For the tests that were performed under visible radiation, LED modules were used, located towards the sides of the reactor. These LED modules emit a continuum spectrum in the wavelength range between 400 and 700 nm with a major peak at 450 nm. The reactor consists of a stirred glass container, with air through a diffuser. The initial concentration of pollutant and catalyst were 20 ppm and 1 g/L, respectively, as in the previous experiments.

Prior to irradiation, in both reactors the suspension was stirred in the dark under air flow for 45 min in order to reach the equilibrium adsorption/desorption. After the adsorption period, an initial sample was extracted to calculate the initial chemical concentration (C_0) and then, the reactor was irradiated in order to start the experimental run. The concentration (C) of AO7 was monitored by measuring the absorbance at 485 nm in a UV-Vis Persee T7DS. The degradation percentage (D) was calculated according to Equation 1:

$$D (\%) = \frac{C_0 - C}{C_0} \times 100 \quad (1)$$

Results and discussion

The obtained XRD diffractogram is shown in **Fig. 1**. From its analysis and later comparison with literature, it can be seen that the MNPs presented the characteristic diffraction peaks for PAA-coated magnetite nanoparticles: $2\theta = 30.2^\circ$, 35.7° , 43.4° , 53.7° , 57.4° , and 62.9° corresponding to Fe_3O_4 nanoparticles and $2\theta = 20^\circ$ for PAA [14]. It is important to remark that the obtaining of pure magnetite cores through a simple procedure represents a clear improvement regarding our previously achieved goals [12].

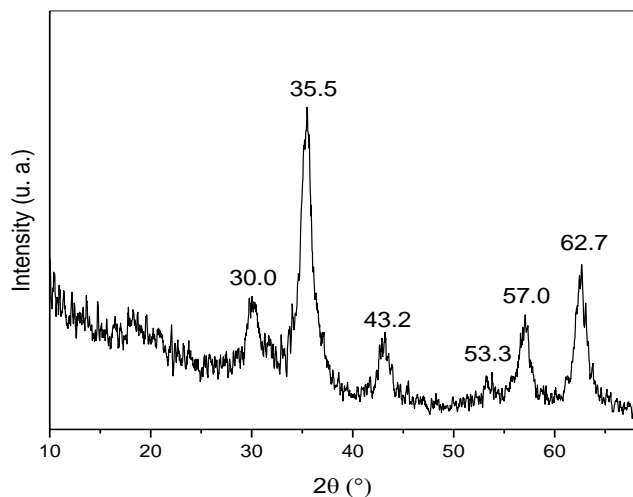


Fig. 1. XRD diffractogram of the MNPs.

Concerning the MNPs quantitative composition, from TGA measurements it was observed that the iron oxides content is near to 75 %. Each weight loss could be associated to a particular event, as have been described in previous reports [14-16]. The initial weight loss is related to the dehydration and decarboxylation of the PAA oligomers. Then, the complete degradation of PAA oligomers could be considered done before 500°C . Finally, the deoxidization of iron oxides takes place at $\sim 700\text{-}750^\circ\text{C}$ and under N_2 atmosphere. The final value at 800°C was taken as the total Iron Oxides mass in the sample.

On the other hand, the hydrodynamic diameters, its distribution and the z-potential in a pH range from 3 to 9

were also determined (**Fig. 2a** and **Fig. 2b**, respectively). The obtained results were in accordance to previously obtained ones for similar MNPs systems [12]. The point zero charge (PZC) is around pH 4. It is worth noting that the PZC reported for raw magnetite nanoparticles is at $\text{pH} = 6.5 - 6.8$ [17]. The shift of the PZC may be considered as an extra proof of the PAA coating on iron oxide nanoparticles. The z-potential values study allows knowing the recommended pH conditions to ensure the best performance for pollutant removal in accordance to its intrinsic charge. Hence, depending on the kind of contaminant, it is feasible to achieve a dual remediation mechanism, i.e. by catalytic degradation or adsorption mediated by electrostatic interactions between the MNPs and the pollutant.

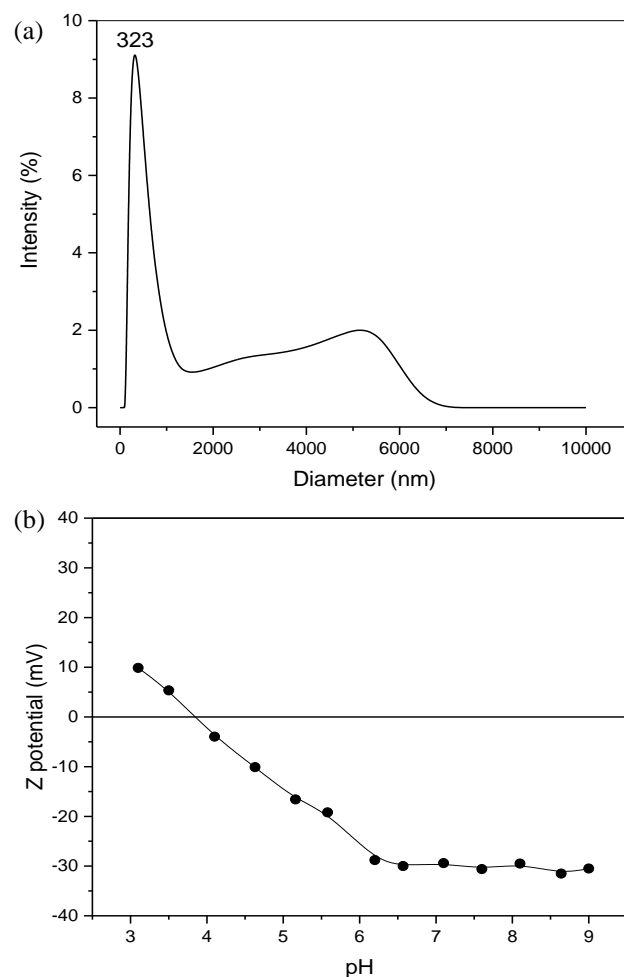


Fig. 2. (a) MNPs sizes distribution determined by dynamic light scattering; (b) MNPs z-potential values as a function of pH.

Regarding the magnetic activity and properties of the prepared PAA-coated MNPs, the obtained results showed a very good response to an external stimulus (**Fig. 3a**), and the measured saturation magnetization is $52.6 (1) \text{ emu/g}$ (**Fig. 3b**). Then, it is possible to remove the MNPs after the water treatments by simply employing a permanent magnet.

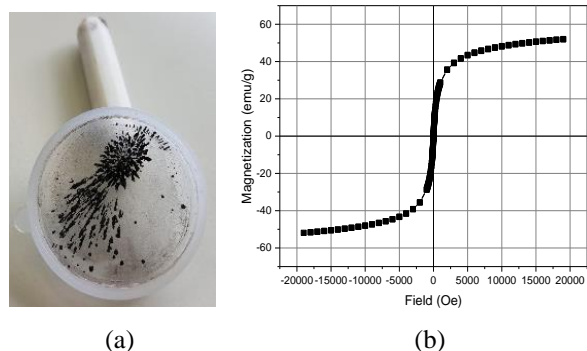


Fig. 3. (a) MNPs response to an external magnetic stimulus. (b) Magnetization per gram of sample as a function of the applied field to the MNPs.

Through the observation of TEM micrographs it is possible to affirm that the iron oxide cores are not agglomerated and their approximate size is around 10 nm (Fig. 4).

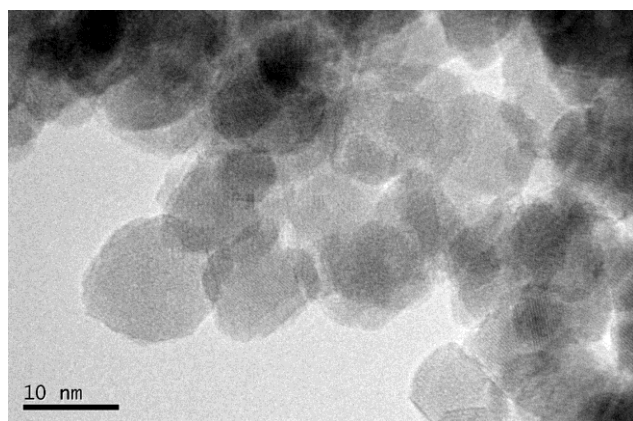
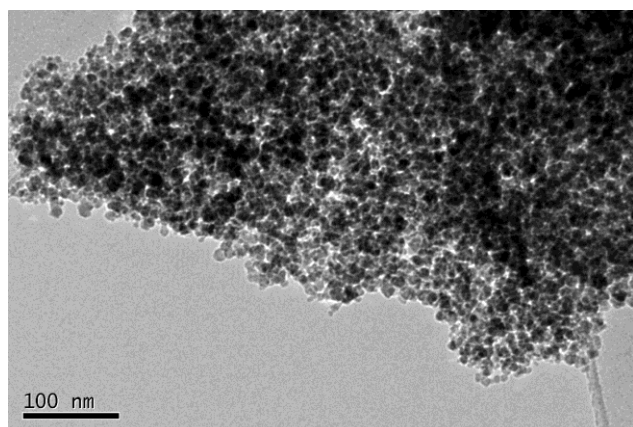


Fig. 4. TEM micrographs of the prepared MNPs.

Finally, AO7 degradation tests were conducted (Table 1). Here no degradation was observed under only UV-Vis radiation (run 4). Then, experiments in order to enhance the activity were performed. Thus, a medium pH adjustment to 3.5 (previous to the catalyst incorporation using a solution of sulfuric acid) as well as the addition of H₂O₂ as oxidant (before exposing the reactor to radiation),

were carried out. For these tests (run 5, 6 and 7) again, no degradation was observed. Nevertheless, under the conditions of Fenton reaction (pH of 3.5 and H₂O₂ addition) the catalyst reaches a notable degradation under both radiations (runs 8 and 9). It has been demonstrated that the prepared material is capable to degrade AO7 being an efficient catalyst even under LED-Vis radiation conditions (Table 1).

Table 1. AO7 degradation tests.

Run	Radiation	H ₂ O ₂ (117 μL)	pH (3.5)	MNPs	Results	
					Degradation (%)	Observations
1	Uv-Vis	Yes	Yes		55	-
2	LED-Vis	Yes	Yes		0	-
3	Uv-Vis		Yes		17	-
4	Uv-Vis			Yes	0	No adsorption
5	Uv-Vis	Yes		Yes	0	No adsorption
6	Uv-Vis		Yes	Yes	0	No adsorption
7	LED-Vis		Yes	Yes	0	No adsorption
8	Uv-Vis	Yes	Yes	Yes	67	5% adsorption
9	LED-Vis	Yes	Yes	Yes	36	7% adsorption

A brief summary of similar Fenton systems recently used for the degradation of dyes is presented in Table 2.

Table 2. Similar Fenton systems intended for the degradation of dyes.

Fenton catalytic system	Dye	Removal efficiency (%)	Reference
Fe ₂ GeS ₄ nanoparticles	Methylene blue	56.3	18
	Methyl orange	66.2	
	Rhodamine blue	74.2	
Magnetic nanoparticles-functionalized carbón (MNPs@C)	Direct Red 16	47*	19
		94.8**	
MNPs coated borosilicate glass	Basic Red 18	82	20

*Using H₂O₂/UV; **UV-Fenton

Conclusion

PAA-coated iron oxide MNPs were successfully prepared through the simple, low-cost and ecofriendly coprecipitation method. The presence of pure non agglomerated Fe₃O₄ cores of approximately 10 nm was

confirmed, being the iron oxides content in the MNPs near to 75%. The magnetization analysis shows that the sample present superparamagnetic response. Regarding the MNPs ability to act as water remediation devices through photo-Fenton processes, the AO7 degradation tests revealed promising results even under LED-Vis radiation conditions.

Future research work will be directed to replace the stabilizing agent in order to diversify the functionality of the MNPs. Furthermore, the target model pollutant will also be changed.

Acknowledgements

The authors acknowledge the financial support of CONICET, ANPCyT and UNMDP.

Keywords

Magnetic nanoparticles, polyacrylic acid, magnetite, photo-fenton reaction.

Received: 20 September 2019

Revised: 04 December 2019

Accepted: 23 December 2019

References

1. Yan, W.; Lien, H. L.; Koel, B. E.; Zhang, W. X.; *Environ. Sci. Process. Impacts*, **2013**, *15*, 63.
2. Litter, M. I.; *Appl. Catal. B Environ.*, **1999**, *23*, 89.
3. Pradeep, T.; Anshup; *Thin Solid Films*, **2009**, *517*, 6441.
4. Akbal, F.; *Environ. Prog.*, **2005**, *24*, 317.
5. Wang, W. Y.; Ku, Y.; *Water Res.*, **2006**, *40*, 2249.
6. Tolba, A.; Alalmd, M. G.; Elsamadonya, M.; Mostafad, A.; Afifya, H.; Dionysiou, D. D.; *Process Saf. Environ. Prot.*, **2019**, *128*, 273.
7. Gonçalves, R. G. L.; Lopes, P. A.; Resende, J. A.; Garcia Pinto, F.; Tronto, J.; Guerreiro, M. C.; Alves de Oliveira, L. C.; de Castro Nunes, W.; Neto, J. L.; *Appl. Clay Sci.*, **2019**, *179*, 105152.
8. Espinosa, J. C.; Catalá, C.; Navalóna, S.; Ferrera, B.; Álvaro, M.; García, H.; *Appl. Catal. B Environ.*, **2018**, *226*, 242.
9. Garole, V. J.; Choudhary, B. C.; Tetgure, S. R.; Garole, D. J.; Borse, A. U.; *Int. J. Environ. Sci. Technol.*, **2018**, *15*, 1649.
10. Sun, Q.; Hong, Y.; Liu, Q.; Dong, L.; *Appl. Surf. Sci.*, **2018**, *430*, 399.
11. Wu, X.; Nan, Z.; *Mater. Chem. Phys.*, **2019**, *227*, 302.
12. Sanchez, L. M.; Martin, D. A.; Alvarez, V. A.; Gonzalez, J. S.; *Colloids Surfaces A Physicochem. Eng. Asp.*, **2018**, *543*, 28.
13. Rutnakornpituk, M.; Puangsin, N.; Theamdee, P.; Rutnakornpituk, B.; Wichai, U.; *Polymer (Guildf)*; **2011**, *52*, 987.
14. Lin, C. L.; Lee, C. F.; Chiu, W. Y.; *J. Colloid Interface Sci.*, **2005**, *291*, 411.
15. Fyfe, C. A.; McKinnon, M. S.; *Macromolecules*, **1986**, *19*, 1909.
16. Schild, H. G.; *J. Polym. Sci. Part A Polym. Chem.*, **1993**, *31*, 2403.
17. Azcona, P.; Zysler, R.; Lassalle, V.; *Colloids Surfaces A Physicochem. Eng. Asp.*, **2016**, *504*, 320.
18. Shi, X.; Tian, A.; You, J.; Yanga, H.; Wang, Y.; Xue, X.; *J. Hazard. Mater.*, **2018**, *353*, 182.
19. Babaei, A. A.; Kakavandi, B.; Rafieed, M.; Kalantarhormizi, I. P.; Ahmadif, E.; Esmailib, S.; *J. Ind. Eng. Chem.*, **2017**, *56*, 163.
20. Ozbey Unal, B.; Bilici, Z.; Ugur, N.; Isik, Z.; Harputluc, E.; Dizgeb, N.; Ocakoglu, K.; *J. Water Process Eng.*, **2019**, *32*, 100897.